JOURNAL OF CHEMICAL & ENGINEERING DATA

ARTICLE

pubs.acs.org/jced

Physicochemical Properties of Ionic Liquids $[C_3py][NTf_2]$ and $[C_6py][NTf_2]$

Qing-Shan Liu,[†] Miao Yang,[†] Pei-Pei Li,[†] Si-Si Sun,[‡] Urs Welz-Biermann,[†] Zhi-Cheng Tan,*[,†,§] and Qing-Guo Zhang*[,‡]

[†]China Ionic Liquid Laboratory, Dalian Institute of Chemical Physics, Chinese Academy of Sciences, Dalian 116023, People's Republic of China

[‡]Department of Chemistry, Bohai University, Jinzhou 121000, People's Republic of China

[§]Thermochemistry Laboratory, Dalian Institute of Chemical Physics, Chinese Academy of Sciences, Dalian 116023, People's Republic of China

Supporting Information

ABSTRACT: Air- and water-stable hydrophobic ionic liquids *N*-alkylpyridinium bis(trifluoromethylsulfonyl)imide ($[C_npy][NTf_2]$, n = 3, 6) were synthesized. The density, surface tension, dynamic viscosity, and electrical conductivity of $[C_6py][NTf_2]$ were measured in the range of T = (283.15 to 338.15) K. The density, dynamic viscosity, and electrical conductivity of $[C_3py][NTf_2]$ were measured in the range of T = (308.15 to 338.15) K. The melting and glass transition temperatures of the two ILs were determined according to the differential scanning calorimetry (DSC). The physicochemical properties, including molecular volume, standard molar entropy, lattice energy, parachor, molar enthalpy of vaporization, interstice volume, interstice fraction, and thermal expansion coefficient, were estimated in terms of empirical and semiempirical equations, as well as the interstice model theory on the base of the experimental values. The dynamic viscosity and electrical conductivity values were fitted by Vogel−Fulcher−Tammann (VFT) and Arrhenius equations for $[C_6py][NTf_2]$ and the Arrhenius equation for $[C_3py][NTf_2]$.

INTRODUCTION

Ionic liquids (ILs) are organic salts that exhibit outstanding physicochemical properties like low melting temperature, good solvation, negligible vapor pressure, high electrical conductivity, and high thermal stability. ILs have received more and more attention as potential green solvents from industrial and scientific communities.[1−4] Most ILs are hydrophilic, so the anion for bis(trifluoromethylsulfonyl)imide $[NTf_2]^-$ ILs as a hydrophobic compound has attracted much more attention in some fields.[5−8] Tokuda et al.[9] have studied the properties of a series of imidazolium-based ILs, for example, the melting temperature, glass transition temperature, dynamic viscosity, and electrical conductivity. The melting temperatures are lower than room temperature, so these ILs are liquid at room temperature; the decomposition temperatures are higher than 690 K, so these ILs exhibit excellent thermal stability. The electrical conductivities are also high enough to be applied in electrochemical devices. Oliveira et al.[10] studied the properties of a series of pyridinium-based ILs. The density and dynamic viscosity of the dried and saturated ILs were studied. The water content has a strong effect on the dynamic viscosity, but only a very small effect on density was observed. Jacquemin et al.[11] have also studied the density and dynamic viscosity of several pure and water-saturated ILs. The same results were obtained for the effect of water content on the density and dynamic viscosity. The ILs with $[NTf_2]^-$ anion were studied widely because this type of ILs has a relatively low viscosity, a wide electrochemical window, and a high electrical conductivity to be applied in the electrochemical devices.[12−16]

In view of the above facts, the density, surface tension, dynamic viscosity, and electrical conductivity of the ILs $[C_npy][NTf_2]$ (n = 3, 6) were measured at different temperatures, except for the surface tension of $[C_3py][NTf_2]$. The speed of sound was estimated by the Auerbach relation at the different temperatures.[17] The standard molar entropy and lattice energy were estimated in terms of Glasser's theory.[18] Parachor was estimated by the equation reported in the ref 19. The molar enthalpy of vaporization was estimated in terms of Kabo's empirical equation.[20] The interstice volume, interstice fraction, and thermal expansion coefficient were estimated by the interstice model theory.[21,22] The Vogel−Fulcher−Tammann (VFT) and Arrhenius equations were used to fit the temperature dependence on dynamic viscosity and electrical conductivity values.

EXPERIMENTAL SECTION

Preparation of ILs $[C_npy][NTf_2]$ (n = 3, 6). *N*-Alkylpyridinium bromide ($[C_npy][Br]$, n = 3, 6) was synthesized according to the procedure described in earlier paper.[23] $[C_npy][NTf_2]$, n = 3, 6, were synthesized according to the ion exchange reaction. The 80 g of salt $[C_npy][Br]$, n = 3, 6 was placed in a 500 mL round-bottomed flask and dissolved in 30 mL of distilled water; the equivalent amount of bis(trifluoromethanesulfonyl)imide ($HN(SO_2CF_3)$) (Rhodia Co., mass purity 99.9 %) was added dropwise

Received: June 1, 2011
Accepted: September 27, 2011
Published: October 17, 2011

Table 1. Molecular Weight and Thermal Properties of ILs $[C_3py][NTf_2]$ and $[C_6py][NTf_2]$

	MW	T_g	T_m
ILs	g·mol^{-1}	K	K
$[C_3py][NTf_2]$	402.33		317.6
$[C_6py][NTf_2]$	444.06	196.6	276.4

Table 2. Mass Fraction, 10^3 w, of Water Before and After the Measurement of Density, Surface Tension, Dynamic Viscosity, and Electrical Conductivity

	$[C_3py][NTf_2]$		$[C_6py][NTf_2]$	
property	before	after	before	after
density	0.18	0.31	0.23	0.45
surface tension			0.23	0.26
viscosity	0.18	0.19	0.23	0.25
conductivity	0.18		0.23	

into the flask at room temperature and stirred for 3 h. The lower liquid was washed several times with 30 mL of distilled water until no Br was present as shown by the solution of $AgNO_3$/HNO_3. The final product was dried under the vacuum at 353 K for 24 h. ^{1}H and ^{13}C NMR spectra were recorded (see Tables 1, 2, and 3 of the Supporting Information). From the NMR, the impurity of the samples was not found. The reaction equations are the following:

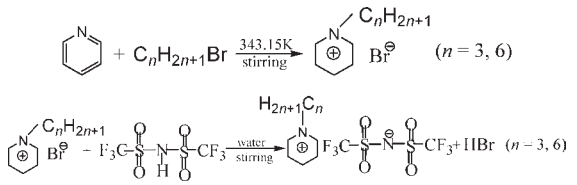

Thermodynamic Property. Differential scanning calorimetry (DSC) was carried out on Q2000 V24.4 Build 116 at a heating rate for 10 K·min^{-1} under nitrogen atmosphere over a temperature window of (153 to 452) K. The data points of the thermal properties in the two samples are listed in Table 1 (aee the Figures A, B of the Supporting Information of DSC).

Water Content. The ILs $[C_npy][NTf_2]$ (n = 3, 6) are hydrophobic compounds. Therefore, the property measurement was carried out at atmospheric pressure except for the electrical conductivity. Since traces of water still exist in the ILs after drying by common methods, the presence of water becomes the most problematic impurity and needs to be confirmed before and after the measurement. The value of the water was the average of the three times measurement by a Cou-Lo Aquamax Karl Fischer moisture meter (v.10.06). The values are listed in Table 2.

Density Measurements. The densities of degassed water were measured by a Westphal balance and the values were in good agreement with the literature[24] within experimental error ± 0.0002 g·cm^{-3}. Then, the densities of the ILs were measured in the temperature range of T = (283.15 to 338.15) ± 0.05 K. The sample was placed in a cell with a jacket. The density values were recorded every 5 K. The temperature was controlled by a thermostat with an uncertainty of ± 0.05 K. The attaining thermal equilibrium time in the cell was 30 min. Each data point of the density is the average value of three measurements. The values are listed in Table 3.

Table 3. Experimental Values of Density, ρ, and Surface Tension, γ, of ILs $[C_3py][NTf_2]$ and $[C_6py][NTf_2]$

	$[C_3py][NTf_2]$		$[C_6py][NTf_2]$			
T	ρ	γ	ρ	ρ^a	ρ^b	γ
K	g·cm^{-3}	mJ·m^{-2}	g·cm^{-3}	g·cm^{-3}	g·cm^{-3}	mJ·m^{-2}
283.15			1.4008	1.4078		32.5
288.15			1.3966	1.4032		32.2
293.15			1.3923	1.3987		32.0
298.15			1.3877	1.3942	1.3865	31.7
303.15			1.3831	1.3897	1.3819	31.6
308.15	1.4845		1.3789	1.3852	1.3774	31.4
313.15	1.4800		1.3744	1.3807	1.3728	31.2
318.15	1.4757		1.3699	1.3763	1.3683	31.0
323.15	1.4710		1.3655	1.3718	1.3638	30.8
328.15	1.4667		1.3615	1.3673	1.3592	30.6
333.15	1.4623		1.3569	1.3629	1.3547	30.3
338.15	1.4574		1.3525	1.3585	1.3502	30.1

[a] The column values are the dried sample experimental values from literature.[30] [b] The column values are the saturated sample experimental values from literature.[30]

Surface Tension Measurements. Using the tensiometer (DP-AW type produced by Sang Li Electronic Co.) of the forced bubble method, the surface tension of the double-distilled freshly degassed water was measured in range of T = (283.15 to 338.15) ± 0.05 K, which is in good agreement with the literature,[24] and the experimental error is ± 0.1 mJ·m^{-2}. The temperature was controlled by a thermostat with an uncertainty of ± 0.05 K. The attaining thermal equilibrium time was 30 min. The surface tension of the samples was measured with the same method. The surface tension values were recorded every 5 K. Each data point of the surface tension is the average value of five measurements. The values of the surface tension of the samples are listed in Table 3.

Dynamic Viscosity Measurements. The dynamic viscosity of the ILs were measured using an Ostwald viscometer within the range of T = (298.15 to 353.15) K. The temperature was controlled by a thermostatic bath with an uncertainty of ± 0.1 K. The attaining thermal equilibrium time in the viscometer was 30 min. The values were recorded every 5 K. Each data point of the viscosity is the average value of three measurements, and the uncertainties were estimated to be ± 1 %. The results are listed in Table 4.

Electrical Conductivity Measurements. The electrical conductivity measurments of the ILs were carried out by a MP522 conductivity instrument with the cell constants of 1 cm^{-1} (the cell was calibrated with the aqueous KCl solution) under the high pure argon gas in the range of T = (283.15 to 338.15) K. The uncertainties were estimated to be ± 1 %. The sample was placed in a cell with a jacket. The temperature was controlled by a thermostat with an uncertainty of ± 0.05 K. The attaining thermal equilibrium time was 30 min. The values were recorded at per 5 K intervals. The results are listed in Table 4.

RESULT AND DISCUSSION

Water Content. Oliveira et al.[10] studied the properties of a series of pyridinium-based ILs. The density and dynamic viscosity of

Table 4. Experimental Values of Electrical Conductivity, η, and Dynamic Viscosity, σ, of ILs $[C_3py][NTf_2]$ and $[C_6py][NTf_2]$

	$[C_3py][NTf_2]$		$[C_6py][NTf_2]$			
T	η	σ	η	η^a	η^b	σ
K	mPa·s	mS·cm^{-1}	mPa·s	mPa·s	mPa·s	mS·cm^{-1}
283.15						0.76
288.15						1.00
293.15						1.30
298.15			84.5	96.206	63.143	1.66
303.15			66.4	75.215	50.410	2.08
308.15	33.0		53.2	59.862	40.912	2.57
313.15	27.6	7.19	43.1	48.419	33.686	3.11
318.15	23.3	8.30	35.2	39.742	28.104	3.87
323.15	19.8	9.55	29.1	33.039	23.728	4.46
328.15	17.1	10.83	24.5	27.794	20.244	5.38
333.15	14.9	12.23	20.9	23.642	17.430	6.21
338.15	13.5	13.65	17.9	20.298	15.157	7.12

[a] The column values are the dried sample experimental values from literature.[30] [b] The column values are the saturated sample experimental values from literature.[30]

the dried and saturated ILs were studied. The water content has strong effect on the dynamic viscosity, but only a very small effect on density was observed. Jacquemin et al.[11] have studied the density and dynamic viscosity of several pure and water-saturated ionic liquids. There is a large change in water content from $0.05 \cdot 10^{-3}$ to $19.8 \cdot 10^{-3}$ mass fraction for the IL $[Emim][NTf_2]$. The values of dynamic viscosity are also changed greatly, for example: the dynamic viscosities are 28.7 mPa·s for dried and 16.8 mPa·s for saturated at 303 K, respectively. The mass fractions of water content are $0.18 \cdot 10^{-3}$ before measurement and $0.19 \cdot 10^{-3}$ after measurement in the present work. The effect of absorbed water in the ILs can be ignored during the measurements.

Thermal Analysis. The glass temperature (T_g), crystallization temperature (T_c), and melting temperature (T_m) can be obtained from the DSC thermograms during the programmed heat/cool/heat step. From the DSC, there are two exothermic peaks for $[C_6py][NTf_2]$ at (231.6 and 243.4) K; it indicated that it has two crystal forms. The inflection value of the glass temperature is T_g = 196.6 K. The peak value of the melting temperature is T_m = 276.4 K; the value is nearly the same as 277 K.[25] The melting point (T_m) of the IL $[C_3py][NTf_2]$ is 317.56 K. The value is much higher than that of 303.61 K for $[C_2py][NTf_2]$,[26] 299.05 K for $[C_4py][NTf_2]$,[26] 272.84 K for $[C_5py][NTf_2]$,[26] and 276.4 K for $[C_6py][NTf_2]$. The temperature dependence on the alkyl chain length of $[C_npy][NTf_2]$ (n = 2, 3, 4, 5, 6) is shown in Figure 1. The melting point of this type ILs $[C_npy][NTf_2]$ (n = 2, 4, 5, 6) is higher than the ILs 1-alkyl-3-methylimidazolium bis(trifluoromethylsulfonyl)imide $[C_nmim][NTf_2]$ (n = 2, 4, 5, 6) that have the same side-chain.[9,27−29] The result can be attributed to the symmetry of the cation that has been demonstrated by Seddon.[30] The melting temperature of $[C_3mim][NTf_2]$ could not be found.[28,29] The melting point of the ILs $[C_npy][NTf_2]$ (n = 2, 3, 4, 5, 6) decreases with the larger the asymmetry of the side chain except for the IL $[C_3py][NTf_2]$. The odd−even effect[31] can be used to explain the result that the melting point

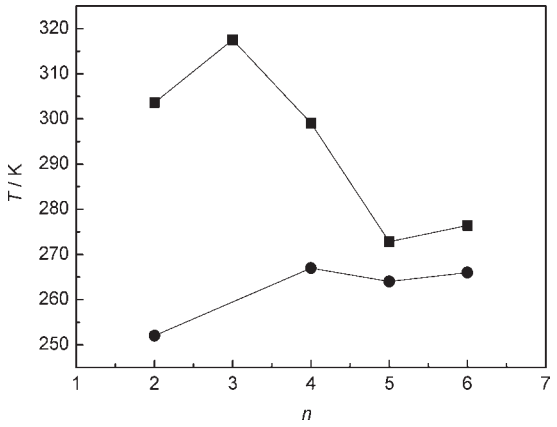

Figure 1. Plot of T_m vs n of ILs: ■, $[C_npy][NTf_2]$ (n = 2, 3, 4, 5, 6); ●, $[C_nmim][NTf_2]$ (n = 2, 4, 5, 6).

Table 5. Estimated Values of Physicochemical Properties of $[C_6py][NTf_2]$ at 298.15 K

property	value	property	value
u/ m·s^{-1}	1095.5	V/cm^{-3}·mol^{-1}	320.2
$10^3 S_a$/ mJ·K^{-1}·m^{-2}	41.82	p	759.9
E_a/ mJ·m^{-2}	44.1	$\Delta_l{}^g H_m{}^0$/ kJ·mol^{-1}	142.9
V_m/nm^3	0.5320	10^{24} v/cm^3	31.77
S^0/ J·K^{-1}·mol^{-1}	692.6	Σv/cm^3	38.25
$10^7 k$/J·K^{-1}	1.316	10^2 $\Sigma v/V$	11.95
T_c/K	1429	10^4 α/K^{-1}, (exp.)	6.40
T_b/K	857	10^4 α/K^{-1}, (cal.)	6.01
U_{pot}/ kJ·mol^{-1}	393		

of $[C_3py][NTf_2]$ is higher than the other ILs $[C_npy][NTf_2]$ (n = 2, 4, 5, 6). So, the asymmetry and odd−even effect lead to the high melting point for IL $[C_3py][NTf_2]$.

Speed of Sound. According to the Auerbach relation,[17] the speed of sound has the following relation with density and surface tension (eq 1). The speed of sound of IL $[C_6py][NTf_2]$ can be estimated by the following equation at 298.15 K.

$$u/\mathrm{m \cdot s^{-1}} = (\gamma/(0.00063\rho))^{2/3} \quad (1)$$

where γ is surface tension, ρ is density, and u is the speed of sound. The estimated value of $[C_6py][NTf_2]$ is listed in Table 5.

Volumetric and Surface Properties. Recently, Oliveira et al.[10] reported the density and dynamic viscosity values of dried and water-saturated IL $[C_6py][NTf_2]$. The values of present work are in the range of the values of the dried and water-saturated IL of the literature. The percent deviations of $[C_6py][NTf_2]$ density of this work with the literature data were determined to be: 0.43 % to 0.48 % for the dried sample, 0.09 % to 0.17 % for the saturated sample; for dynamic viscosity: 12 % to 14 % for the dried sample; 15 % to 25 % for the saturated sample. As expected, the temperature dependence on the density and surface tension in the range of the measurement can be fitted by the following equation:

$$Y = A + BT + CT^2 \quad (2)$$

where Y is the density or surface tension; A, B, and C are adjustable parameters. The fitting curve can be obtained (see

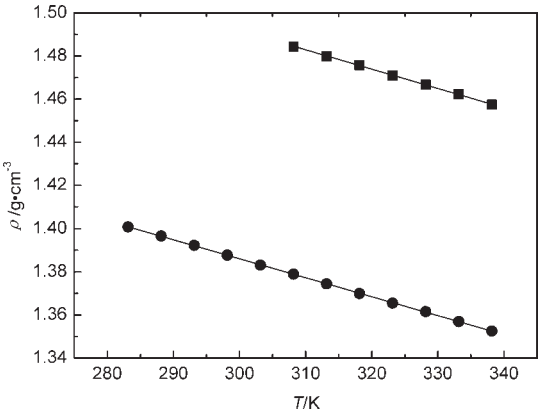

Figure 2. Plot of density, ρ, vs T/K: ■, $[C_3py][NTf_2]$; ●, $[C_6py][NTf_2]$.

Table 6. Fitting Parameters and Correlation Coefficient for Density and Surface Tension

ILs	property	A	$10^4\,B$	$10^7\,C$	R^2
$[C_3py][NTf_2]$	ρ/g·cm^{-3}	1.6768	−3.7466	−8.0952	0.9998
	γ/mJ·m^{-2}				
$[C_6py][NTf_2]$	ρ/g·cm^{-3}	1.6655	−9.7932	1.5884	0.9999
	γ/mJ·m^{-2}	43.5	368.5	−0.7992	0.9952

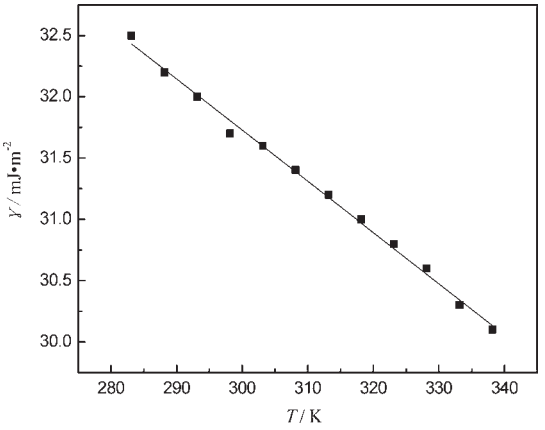

Figure 3. Plot of surface tension, γ vs T/K: ■, $[C_6py][NTf_2]$.

Figure 2). The best fitting values and the correlation coefficient are listed in Table 6.

By plotting the ln ρ against T/K, a straight line can be obtained, and the empirical equation is:

$$\ln \rho/\mathrm{g\cdot cm^{-3}} = b - \alpha \cdot T/\mathrm{K} \quad (3)$$

where b is an empirical constant and the negative value of the slope, $\alpha = -(\partial \ln \rho/\partial T)_p$, is the thermal expansion coefficient of the sample. The fitted equation is ln ρ/g·cm^{-3} = 0.5183 − $6.40\cdot10^{-4}T$/K for $[C_6py][NTf_2]$, R^2 = 0.9999. So, the thermal expansion coefficient is $6.40\cdot10^{-4}$ K^{-1} for $[C_6py][NTf_2]$.

For $[C_6py][NTf_2]$, by plotting the values of γ obtained from the experiment against T/K, a linear equation was obtained (see Figure 3). From Figure 3, the surface entropy, $S_a = -(\partial\gamma/\partial T)_p$, can be obtained, and the value is $41.82\cdot10^{-3}$ mJ·K^{-1}·m^{-2}.

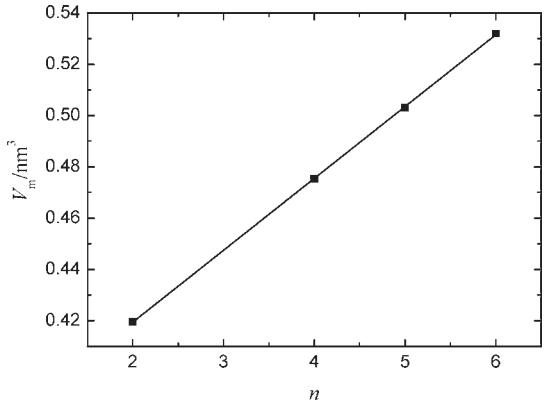

Figure 4. Plot of V_m vs n at 298.15 K. The correlation coefficient is R^2 = 0.9999.

Table 7. Estimated Volumetric Properties of the ILs $[C_npy][NTf_2]$ (n = 2, 4, 5, 6) at 298.15 K

	ρ	V_m		V_+	r_+
	g·cm^{-3}	nm^3	M_+	nm^3	nm
$[C_2py][NTf_2]$[a]	1.5375	0.4196	108.16	0.2164	0.372
$[C_4py][NTf_2]$[a]	1.4547	0.4754	136.22	0.2722	0.402
$[C_5py][NTf_2]$[a]	1.4214	0.5030	150.24	0.2998	0.415
$[C_6py][NTf_2]$[b]	1.3877	0.5320	164.27	0.3288	0.428

[a] Reference 25. [b] This work.

Additionally, the surface energy, $E_a = \gamma - T(\partial\gamma/\partial T)_p$, can be estimated by the experimental value of the surface tension; the value of $[C_6py][NTf_2]$ is 44.1 mJ·m^{-2}. Comparing with fused salts and organic liquids, this value is lower than fused salts, for example, E_a = 146 mJ·m^{-2} for $NaNO_3$, and is closed to organic liquids, for example, E_a = 67 mJ·m^{-2} for benzene and E_a = 51.1 mJ·m^{-2} for octane.[32] This fact shows that the alkyl group of the ionic liquid at the liquid/vapor interface is directed toward the vapor.

The molecular volume, V_m, can be calculated from experimental density using the following equation:

$$V_m(298.15\mathrm{K}) = M/(N\cdot\rho) \quad (4)$$

where M is molar mass, ρ is density, and N is Avogadro's constant. The values of the molecular volume are 0.5320 nm^3 for $[C_6py][NTf_2]$, 0.4196 nm^3 for $[C_2py][NTf_2]$, 0.4754 nm^3 for $[C_4py][NTf_2]$, and 0.5030 nm^3 for $[C_5py][NTf_2]$ at 298.15 K.[26] The plot of V_m against the number of the carbons, n, in the alkyl chain of the samples ($[C_npy][NTf_2]$) can be obtained (see Figure 4). The value, 0.0280 nm^3, of the slope of the fitting line is the mean contribution of the methylene to the molecular volume at 298.15 K. It is close to the values of 0.0272 nm^3 for ILs $[C_nmim][BF_4]$,[18] 0.0282 nm^3 for $[C_nmim][NTf_2]$,[18] and 0.0278 nm^3 for $[C_nmim][Ala]$.[33] The molar mass of cations of the ILs $[C_npy][NTf_2]$ (n = 2, 4, 5, 6) was listed in Table 7. The plot of V_m against the molar mass of cations of the samples ($[C_npy][NTf_2]$) can be obtained. The intercept of the linear regression can be approximately regarded by the volume of the anion, NTf_2^-; the value is 0.2032 nm^3. The volume value of NTf_2^- is much higher than 0.1390 nm^3 for $AlCl_4^-$[34] and

dx.doi.org/10.1021/je200534b |J. Chem. Eng. Data 2011, 56, 4094–4101

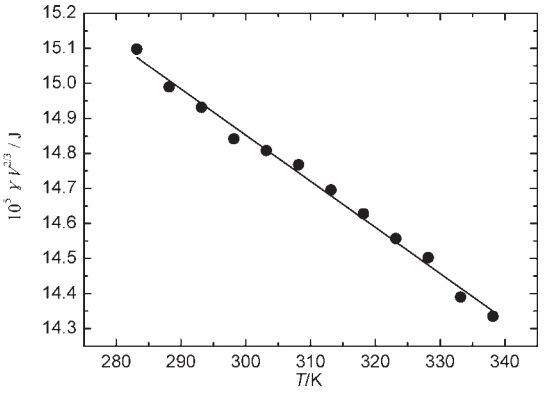

Figure 5. Plot of $\gamma V_m^{2/3}$ vs T (K). The correlation coefficient is R^2 = 0.9918. ●, $[C_6py][NTf_2]$.

0.1548 nm^3 $GaCl_4^-$.[35] The volume values of the cations and the radii are listed in Table 7.

According to Glasser's theory,[18] the standard molar entropy can be estimated from the equation:

$$S^0(298.15K)/J\cdot K^{-1}\cdot mol^{-1} = 1246.5(V_m/nm^3) + 29.5 \quad (5)$$

where V_m is the molecular volume. The value of $[C_6py][NTf_2]$ is listed in Table 5.

The surface tension, γ, has a relationship with the temperature in terms of the Eötvös equation:[32]

$$\gamma V_m^{2/3} = k(T_c - T) \quad (6)$$

where V is the molar volume of the liquid, T_c is the critical temperature, and k is an empirical constant.

The water mass fractions of $[C_6py][NTf_2]$ are $0.23\cdot10^{-3}$ before measurement and $0.26\cdot10^{-3}$ after measurement of the surface tension in the present work. The water content mass fraction increases by 13 % during the measurement. The effect of absorbed water in the ILs on surface tension during the measurements can be evaluated from the fluctuation around the linear fit (with R^2 = 0.9918) seen in Figure 5. Customarily, a fit with a correlation coefficient larger than 0.995 is considered a good fit. By plotting the $\gamma V_m^{2/3}$ of $[C_6py][NTf_2]$ against T, a straight line was obtained (see Figure 5). From the plot, the value of empirical constant (k) and critical temperature (T_c) can be obtained according to the fitting equation. The values of $k = 1.316\cdot10^{-7}$ $J\cdot K^{-1}$ and T_c = 1429 K were obtained. Rebole et al.[36] have reported that the normal boiling point, T_b, is approximately $0.6T_c$ for ILs. Herein, the normal boiling point, T_b, can be calculated, and the value is T_b = 857 K. For the majority of organic liquids, $k \approx 2.1\cdot10^{-7}$ $J\cdot K^{-1}$, but for fused salts, $k = 0.4\cdot10^{-7}$ $J\cdot K^{-1}$ for fused NaCl.[32] It indicated that $[C_6py][NTf_2]$ has a medium polarity between organic liquids and fused salts in terms of the value of k.

The lattice energy, U_{POT}, was estimated according to the following equation:[18]

$$U_{POT}(298.15K)/kJ\cdot mol^{-1} = 1981.2(\rho/M)^{1/3} + 103.8 \quad (7)$$

where M is molar mass and ρ is the density.

All of the data obtained from the empirical and semiempirical equations are listed in Table 5.

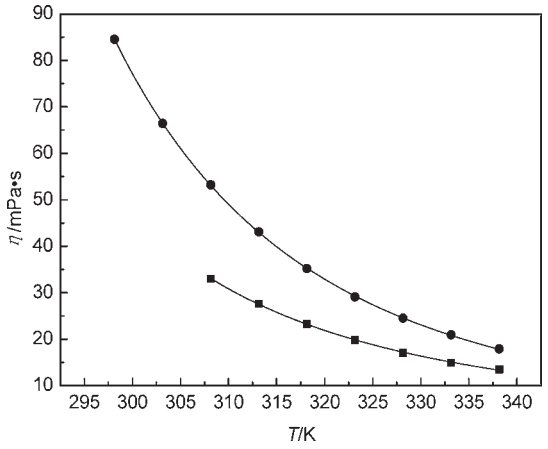

Figure 6. Plot of dynamic viscosity, η, vs T/K: ■, $[C_3py][NTf_2]$; ●, $[C_6py][NTf_2]$.

Parachors and Molar Enthalpy of Vaporization. The parachor, P, was estimated from the following equation:[19]

$$P(298.15K) = (M\cdot\gamma^{1/4})/\rho \quad (8)$$

where M is molar mass, ρ is density, and γ is surface tension.

The value of molar enthalpy of vaporization was estimated in terms of Kabo's empirical equation:[20]

$$\Delta_l^g H_m^0(298.15K)/kJ\cdot mol^{-1} = 0.01121(\gamma V^{2/3}\cdot N^{1/3}) + 2.4 \quad (9)$$

where V is molar volume, γ is surface tension, and N is Avogadro's constant.

The data of parachor and molar enthalpy of vaporization are listed in Table 5.

Interstice Model Theory. According to the interstice model,[21,22] the interstice volume, v, can be estimated by classical statistical mechanics:

$$v = 0.6791(k_b\cdot T/\gamma)^{3/2} \quad (10)$$

where k_b is Boltzmann constant, T is the thermodynamic temperature, and γ is the surface tension of ILs.

The molar volume of ionic liquids, V, consists of the inherent volume, V_i, and the volume of the interstices; the molar volume of the interstice, $\Sigma v = 2N\cdot v$:

$$V = V_i + 2N\cdot v \quad (11)$$

If the expansion volume of IL only results from the expansion of the interstices when the temperature increases, the thermal expansion coefficient, α, can be predicted from the interstice model:

$$\alpha = (1/V)(\partial V/\partial T)_p = 3N\cdot v/(V\cdot T) \quad (12)$$

All of the data obtained from the empirical and semiempirical equations are listed in Table 5

From Table 5, the value of estimation of the thermal expansion coefficient is in good agreement with experimental value. It also can be seen that the estimated value of interstice fraction, $\Sigma v/V$, is 11.95 % for $[C_6py][NTf_2]$; the value is in good agreement with the values of volume expansion resulted in the process from solid to liquid state for majority materials which exhibit (10 to 15) %.

Table 8. Fitted Values of Electrical Conductivity, Dynamic Viscosity, and Molar Conductivity of σ_∞, E_σ, σ_0, η_∞, E_η, η_0, Λ_0, B, T_0, and R According to the VFT and Arrhenius Equations

		Arrhenius equation			VFT equation			
		$10^4\eta_\infty$	E_η		η_0	B	T_0	
property	IL	mPa·s	kJ·mol^{-1}	R^2	mPa·s	K	K	R^2
η/ mPa·s	$[C_3py][NTf_2]$	11.77	26.19	0.9957				
	$[C_6py][NTf_2]$	1.65	32.51	0.9984	0.0645	1036.0	153.8	0.9999
		$10\sigma_\infty$/S·cm^{-1}	E_σ/kJ·mol^{-1}	R^2	σ_0/S·cm^{-1}	B/K	T_0/K	R^2
σ/mS·cm^{-1}	$[C_3py][NTf_2]$	4.31	22.63	0.9991				
	$[C_6py][NTf_2]$	77.95	32.44	0.9970	0.81	803.1	168.4	0.9996
					$10^{-2}\Lambda_0$/ S·cm^2·mol^{-1}	B/K	T_0/K	R^2
Λ/ S·cm^2·mol^{-1}	$[C_6py][NTf_2]$				3.14	841.7	166.2	0.9996

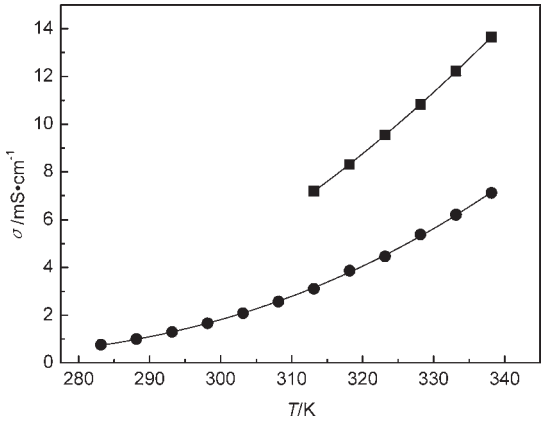

Figure 7. Plot of electrical conductivity, σ, vs T/K: ■, $[C_3py][NTf_2]$; ●, $[C_6py][NTf_2]$.

This means that the interstice model is reasonable and the interstice model theory can be applied to calculate the thermal expansion coefficient of pyrinidium-based ILs.

The temperature dependence on dynamic viscosity was plotted for ILs $[C_npy][NTf_2]$ (n = 3, 6) (see Figure 6). By fitting ln η against T^{-1}, a fitting equation can be obtained according to the Arrhenius equation, and the Arrhenius equation is:[12,37]

$$\ln \eta = \ln \eta_\infty + E_\eta/(R \cdot T) \quad (13)$$

where η is dynamic viscosity, η_∞ is an empirical constant, and E_η is the activation energy for viscous flow. The values of η_∞, E_η, and correlation coefficient, R^2, are listed in Table 8.

The values of dynamic viscosity of ILs $[C_6py][NTf_2]$ were fitted by using the Vogel−Fulcher−Tamman (VFT) equation, which is commonly used for ILs:[9,38,39]

$$\eta = \eta_0 \exp(B/(T - T_0)) \quad (14)$$

where η_0, B, and T_0 are empirical constants. The best fit values of η_0, B, and T_0 and the correlation coefficient, R^2, are listed in Table 8.

The temperature dependence on electrical conductivity was studied for ILs $[C_npy][NTf_2]$ (n = 3, 6) (see Figure 7). By fitting ln σ against T^{-1}, a fitting equation can be obtained according to the Arrhenius equation:[39]

$$\ln \sigma = \ln \sigma_\infty - E_\sigma/(RT) \quad (15)$$

where σ is conductivity, σ_∞ is an empirical constant, and E_σ is the activation energy for electrical conduction (which indicates the energy for an ion jump to a free hole). The values of σ_∞, E_σ, and correlation coefficient, R^2, are listed in Table 8.

The values of electrical conductivity of ILs $[C_6py][NTf_2]$ were fitted by using the Fulcher equation, which is commonly used for ILs:[9,38,39]

$$\sigma = \sigma_0 \exp(-B/(T - T_0)) \quad (16)$$

where σ_0, B, and T_0 are empirical constants. The best fit values of σ_0, B, and T_0 and the correlation coefficient, R^2, are listed in Table 8.

From Table 8, the values of the correlation coefficient, R, of the IL $[C_6py][NTf_2]$ based on the VFT equation are better than that from the Arrhenius equation. The VFT equation can be considered to be more suitable for application to ILs than the Arrhenius equation. The dynamic viscosity and conductivity of the IL $[C_3py][NTf_2]$ were not fitted by the VFT equation within the narrow temperature range from (308.15 to 338.15) K.

From Table 8, it can be seen that the activation energies of dynamic viscosity and conductivity are increased with the extension of the alkyl side chain of the cation; the discrepancies between the activation energies of dynamic viscosity and electrical conductivity are relatively small. Hagiwara et al.[40] obtained the same result; it suggests that the high conductivity can be explained by the low viscosity without introducing some special conduction mechanism such as ion hopping.

The molar conductivity was calculated according to the following equation:

$$\Lambda = \sigma \cdot M \cdot \rho^{-1} \quad (17)$$

where Λ is the molar conductivity, σ is the conductivity, M is the molar mass, and ρ is the density. The values of the molar conductivity are listed in Table 9. The temperature dependence on molar conductivity of $[C_6py][NTf_2]$ was also fitted according to the VFT equation:

$$\Lambda = \Lambda_0 \exp(-B/(T - T_0)) \quad (18)$$

dx.doi.org/10.1021/je200534b |J. Chem. Eng. Data 2011, 56, 4094–4101

Table 9. Molar Conductivity, Λ, of ILs $[C_npy][NTf_2]$ (n = 3, 6)

	Λ/ S·cm²·mol⁻¹					
T/K	283.15	288.15	293.15	298.15	303.15	308.15
$[C_3py][NTf_2]$						
$[C_6py][NTf_2]$	0.24	0.32	0.41	0.53	0.67	0.83
T/K	313.15	318.15	323.15	328.15	333.15	338.15
$[C_3py][NTf_2]$	1.95	2.26	2.61	2.97	3.36	3.77
$[C_6py][NTf_2]$	1.00	1.25	1.45	1.75	2.03	2.34

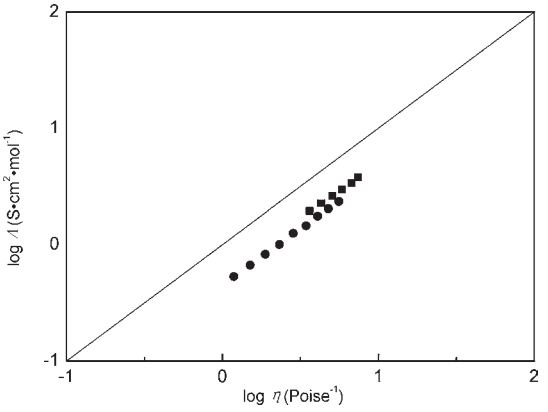

Figure 8. Walden plots for ILs $[C_npy][NTf_2]$ (n = 3, 6) at temperatures from (298.15 to 338.15) K: ■, $[C_3py][NTf_2]$; ●, $[C_6py][NTf_2]$; the solid straight line is the ideal line for a 0.01 M aqueous KCl solution.

where Λ, B, and T_0 are constants. The best-fitted parameters are listed in Table 8.

The relationship of the molar conductivity and dynamic viscosity has been described by the Walden rule:[41−44]

$$\Lambda\eta = k \tag{19}$$

where Λ is the molar conductivity, η is the dynamic viscosity, and k is a temperature-dependent constant. The Walden products (in $[S\cdot cm^2\cdot mol^{-1}][cP]$) are 54 for $[C_3py][NTf_2]$ at 318.15 K, 45 for $[C_6py][NTf_2]$ at 298.15 K, and 44 for $[C_6py][NTf_2]$ at 318.15 K, respectively.

Log Λ dependence on log η^{-1} were ploted for ILs $[C_npy][NTf_2]$ (n = 3, 4) from (298.15 to 338.15) K (see Figure 8). From Figure 8, the curves approximate to straight lines, which indicates that the ILs obey the Walden rule. The position of the ideal line was established using aqueous KCl solutions at high dilution. The lines for ILs $[C_npy][NTf_2]$ (n = 3, 6) below lie closely to the ideal KCl line. Most of the ILs have the same tendency.[41−47] The slopes of the lines for ILs $[C_3py][NTf_2]$ and $[C_6py][NTf_2]$ are 0.906 and 0.959, respectively. The result indicates that the conductivity fluidity relationship remains constant.

CONCLUSIONS

The IL $[C_6py][NTf_2]$ has two crystal forms from DSC. The inflection value of the glass temperature is T_g = 196.6 K. The melting temperature is T_m = 276.4 K. The melting point of the IL $[C_3py][NTf_2]$ is 317.56 K. The asymmetry and odd effect lead to the melting temperature of the IL $[C_3py][NTf_2]$, which is higher than the IL $[C_npy][NTf_2]$ (n = 2, 4, 5, 6). The effect of temperature on density, surface tension, dynamic viscosity, and electrical conductivity values of $[C_npy][NTf_2]$ (n = 3, 6) were experimentally determined except for the surface tension of $[C_3py][NTf_2]$. The properties of the IL $[C_6py][NTf_2]$ were calculated by the empirical and semiempirical equations. The VFT and Arrhenius equations were used to fit the dynamic viscosity and electrical conductivity values on temperature. The activation energies of visicous flow and electrical conduction were obtained according to the Arrhenius equation. The values increase with the extension of the alkyl side chain of the cation. The relationship of the molar conductivity and dynamic viscosity was described by the Walden rule.

ASSOCIATED CONTENT

Supporting Information. ^{1}H NMR spectral data pf C_6pyrBr (Table 1) and $[C_3py][NTf_2]$ amd $[C_6py][NTf_2]$ (Table 2) in DMSO and ^{13}C NMR spectral data of $[C_3py][NTf_2]$ amd $[C_6py][NTf_2]$ in DMSO (Table 3); DSC curves of $[C_3py][NTf_2]$ amd $[C_6py][NTf_2]$ (Figures A and B, respectively). This material is available free of charge via the Internet at http://pubs.acs.org.

AUTHOR INFORMATION

Corresponding Author

*E-mail: tzc@dicp.ac.cn (Z.-C. Tan).

Funding Sources

This work was financially supported by the National Nature Science Foundation of China under Grant NSFC Nos. 21073189, 20901076, and 21003081 and the Knowledge Innovation Program of the Chinese Academy of Sciences under Grant DICP K2009D03.

REFERENCES

(1) Rantwijk, F. V.; Sheldon, R. A. Biocatalysis in ionic liquids. *Chem. Rev.* **2007**, *107*, 2757–2785.

(2) Greaves, T. L.; Drummond, C. J. Protic Ionic Liquids: Properties and Applications. *Chem. Rev.* **2008**, *108*, 206–237.

(3) Hapiot, P.; Lagrost, C. Electrochemical Reactivity in Room-Temperature Ionic Liquids. *Chem. Rev.* **2008**, *108*, 2238–2264.

(4) Jessop, P. G.; Subramaniam, B. Gas-Expanded Liquids. *Chem. Rev.* **2007**, *107*, 2666–2694.

(5) Kim, G. T.; Appetecchi, G. B.; Alessandrini, F.; Passerini, S. Solvent-free, PYR_{1A}TFSI ionic liquid-based ternary polymer electrolyte systems I. Electrochemical characterization. *J. Power Sources* **2007**, *171*, 861–869.

(6) Orita, A.; Kamijima, K.; Yoshida, M.; Yang, L. Application of sulfonium-, and thioxonium-based salts as electric double-layer capacitor electrolytes. *J. Power Sources* **2010**, *195*, 6970–6976.

(7) Lazzari, M.; Mastragostino, M.; Pandolfo, A. G.; Ruiz, V.; Soavi, F. Role of Carbon Porosity and Ion Size in the Development of Ionic Liquid based Supercapacitors. *J. Electrochem. Soc.* **2011**, *158* (1), A22–A25.

(8) Orita, A.; Kamijima, K.; Yoshida, M. Allyl-functionalized ionic liquids as electrolytes for electric double-layer capacitors. *J. Power Sources* **2010**, *195*, 7471–7479.

(9) (a) Tokuda, H.; Hayamizu, K.; Ishii, K.; Susan, M. A. B. H.; Watanabe, M. Physicochemical properties and structures of room temperature ionic liquids. 2. Variation of alkyl chain length in imidazolium cation. *J. Phys. Chem. B* **2005**, *109*, 6103–6110. (b) Tokuda, H.; Tsuzuki, S.; Susan, M. A. B. H.; Hayamizu, K.; Watanabe, M. How Ionic Are Room-Temperature Ionic liquids? An Indicator of the Physicochemical Properties. *J. Phys. Chem. B* **2006**, *110*, 19593–19600.

(10) Oliveira, F. S.; Freire, M. G.; Xarvalho, P. J.; Coutinho, J. A. P.; Lopes, J. N. C.; Rebelo, L. P. N.; Marrucho, I. M. Structural and

Positional Isomerism Infulence in the Physical Properties of Pyridinium NTf_2-Based Ionic Liquids: Pure and Water-Saturated Mixtures. *J. Chem. Eng. Data* **2010**, *55*, 4514–4520.

(11) Jacquemin, J.; Husson, P.; Padua, A. A. H.; Majer, V. Density and viscosity of several pure and water-saturated ionic liquids. *Green Chem.* **2006**, *8*, 172–180.

(12) Fang, S. H.; Yang, L.; Wei, C.; Peng, C. X.; Tachibana, K.; Kamijima, K. Low-viscosity and low-melting point asymmetric trialkylsulfonium based ionic liquids as potential electrolytes. *Electrochem. Commun.* **2007**, *9*, 2696–2702.

(13) Kazock, J.; Taggougui, M.; Anouti, M.; Willman, P.; Carré, B.; Lemordant, D. Ionic liquids based on 1-aza-bicyclo[2,2,2]cotane (quinuclidine)salts: synthesis and physicochemical properties. *J. Appl. Electrochem.* **2009**, *39*, 2461–2467.

(14) Sakaebe, H.; Matsumoto, H. *N*-methyl-*N*-propylpiperdinium bis(trifluoromethanesulfonyl)imide (PP13-TFSI)—novel electrolyte base for Li battery. *Electrochem. Commun.* **2003**, *5*, 594–598.

(15) Yang, L.; Zhang, Z. X.; Gao, X. H.; Zhang, H. Q.; Mashita, K. Asymmetric sulfonium-based molten salts with $TFSI^-$ or PF_6 anion as novel electrolytes. *J. Power Sources* **2006**, *162*, 614–619.

(16) Matsumoto, H.; Sakaebe, H.; Tatsumi, K.; Kikuta, M.; Ishiko, E.; Kono, M. Fast cycling of Li/$LiCoO_2$ cell with low-viscosity ionic liquids based on bis(fluorosulfony)imide[$FSI]^-$. *J. Power Sources* **2006**, *160*, 1308–1303.

(17) Bandr, I.; Giner, B.; Artigas, H.; Royo, F. M.; Lafuente, C. Thermophysic comparative study of two isomeric pyridinium-based ionic liquids. *J. Phys. Chem. B* **2008**, *112*, 3077–3084.

(18) Glasser, L. Lattice and phase transition thermodynamics of ionic liquids. *Thermochim. Acta* **2004**, *421*, 87–93.

(19) Deetlefs, M.; Seddon, K. R.; Shara, M. Predicting physical properties of ionic liquids. *Phys. Chem. Chem. Phys.* **2006**, *8*, 642–649.

(20) Zaitsau, D. H.; Kabo, G. J.; Strechan, A. A.; Paulechka, Y. U.; Tschersich, A.; Verevkin, S. P.; Heintz, A. Experimental vapor pressures of 1-alkyl-3-methylimidazolium bis(trifluoromethylsulfonyl)imides and a correlation scheme for estimation of vaporization enthalpies of ionic liquids. *J. Phys. Chem. A* **2006**, *110*, 7303–7306.

(21) Yang, J. Z.; Lu, X. M.; Gui, J. S.; Xu, W. G. A new theory for ionic liquids-the interstice model part1. The density and surface tension of ionic liquid EMISE. *Green Chem.* **2004**, *6*, 541–543.

(22) Zhang, Q. G.; Yang, J. Z.; Lu, X. M.; Gui, J. S.; Huang, M. Study on an ionic liquid based on $FeCl_3$ and its properties. *Fluid Phase Equilib.* **2004**, *226*, 207–211.

(23) Tong, B.; Liu, Q. S.; Tan, Z. C.; Welz-Biermann, U. Thermochemistry of alkyl pyridinium bromide ionic liquids: Calorimetric measurements and calculations. *J. Phys. Chem. A* **2010**, *114*, 3782–3787.

(24) Lide, D. R. *Handbook of Chemistry and Physics*, 82nd ed.; CRC Press: Boca Raton, 2001—2002.

(25) http://www.aails.com/ilc_det.asp?sort=hpyrntf.

(26) Liu, Q. S.; Yang, M.; Yan, P. F.; Liu, X. M.; Tan, Z. C.; Welz-Biermann, U. Density and surface tension of ionic liquids [$C_n$py][NTf_2] (n = 2, 4, 5). *J. Chem. Eng. Data* **2010**, *55*, 4928–4930.

(27) Dzyuba, S. V.; Bartsch, R. A. Influence of structural variations in 1-alkyl(aralkyl)-3-methylimidazolium hexafluorophosphates and bis-(trifluoromethyl-sulfonyl)imides on physical properties of the ionic liquids. *Chem. Phys. Chem.* **2002**, *3*, 161–166.

(28) Ngo, H. L.; LeCompte, K.; Hargens, L.; McEwen, A. B. Thermal properties of imidazolium ionic liquids. *Thermochim. Acta* **2000**, *357—358*, 97–102.

(29) Klubek, G.; Yu, Y.; Krause-Rehberg, R.; Beichel, W.; Bulut, S.; Pogodina, N.; Krossing, I.; Friedrich, C. Free volume in imidazolium triflimide ([C_3MIM][NTf_2]) ionic liquid from positron lifetime: Amorphous, crystalline, and liquid states. *J. Chem. Phys.* **2010**, *133*, 124502/1–124502/10.

(30) Seddon, K. R. Ionic liquids for clean technology. *J. Chem. Technol. Biotechnol.* **1970**, *68*, 351–356.

(31) Holbrey, J. D.; Seddon, K. T. The phase behaviour of 1-alkyl-3-methylimidazolium tetrafluoroborates; ionic liquids and ionic liquid crystals. *J. Chem. Soc., Dalton Trans.* **1999**, 2133–2139.

(32) Adamson, A. W. *Physical chemistry of surfaces*, 3rd ed.; John-Wiley: New York, 1976; translated by Gu, T. R.; Science Press: Beijing, 1986.

(33) Fang, D. W.; Guan, W.; Tong, J.; Wang, Z. W.; Yang, J. Z. Study on physicochemical properties of ionic liquids based on alanine [$C_n$mim][Ala] (n = 2, 3, 4, 5, 6). *J. Phys. Chem. B* **2008**, *112* (25), 7499–7505.

(34) Tong, J.; Hong, M.; Guan, W.; Yang, J. Z. Studies on the thermodynamic properties of new ionic liquids: 1-Methyl-3-pentylimidazolium salts containing metal of group III. *J. Chem. Thermodyn.* **2006**, *38*, 1416–1421.

(35) Tong, J.; Liu, Q. S.; Guan, W.; Yang, J. Z. Estimation of Physicochemical Properties of Ionic Liquid C_6MIGaCl_4 Using Surface Tension and Density. *J. Phys. Chem. B* **2007**, *111*, 3197–3200.

(36) Rebelo, L. P. N.; Lopes, J. N. C.; Esperança, J. M. S. S.; Filipe, E. On the critical temperature, normal boiling point, and vapor pressure of ionic liquids. *J. Phys. Chem. B* **2005**, *109*, 6040–4386.

(37) Bonhôte, P.; Dias, A. P.; Papageorgiou, N.; Kalyanasundaram, K.; Grätzel, M. Hydrophobic, highly comductive ambient-temperature molten salts. *Inorg. Chem.* **1996**, *35*, 1168–1178.

(38) Wu, T. Y.; Su, S. G.; Gung, S. T.; Lin, M. W.; Lin, Y. C.; Lai, C. A.; Sun, I. W. Ionic liquids containing an alkyl sulfate group as potential electrolytes. *Electrochim. Acta* **2010**, *55*, 4475–4482.

(39) Carpio, R. A.; King, L. A.; Kibler, F. C., Jr.; Fannin, A. A., Jr. Conductivities of $AlCl_3$-LiCl mixtures. *J. Electrochem. Soc.* **1979**, *126*, 1650–1654.

(40) Hagiwara, R.; Matsumoto, K.; Nakamori, Y.; Tsuda, T.; Ito, Y.; Matsumoto, H.; Momota, K. Physicochemical Properties of 1,3-Dialkylimidazolium Fluorohydrogenate Room-Temperature Molten Salts. *J. Electrochem. Soc.* **2003**, *150*, D195–D199.

(41) Yoshizawa, M.; Xu, W.; Angell, C. A. Ionic Liquids by Proton Trasfer: Vapor Pressure, Conductivity, and the Relevance of ΔpK_a from Aqueous Solutions. *J. Am. Chem. Soc.* **2003**, *125*, 15411–15419.

(42) Angell, C. A.; Byrne, N.; Belieres, J. P. Parallel Developments in Aprotic and Protic Ionic liquids: Physical Chemistry and Applications. *Acc. Chem. Res.* **2007**, *40*, 1228–1236.

(43) Xu, W.; Cooper, E. I.; Angell, C. A. Ionic Liquids: Ion Mobilities, Glass Temperatures, and Fragilities. *J. Phys. Chem. B* **2003**, *107*, 6170–6178.

(44) MacFarlane, D. R.; Forsyth, M.; Izgorodina, E. I.; Abbott, A. P.; Annat, G.; Fraser, K. On the concept of ionicity in ionic liquids. *Phys. Chem. Chem. Phys.* **2009**, *11*, 4962–4967.

(45) Xu, W.; Wang, L. M.; Nieman, R. A.; Angell, C. A. Ionic Liquids of Chelated Orthoborates as Model Ionic Glassformers. *J. Phys. Chem. B* **2003**, *107*, 11749–11756.

(46) Fraser, K. J.; Izgorodina, E. I.; Forsyth, M.; Scott, J. L.; MacFarlane, D. R. Liquids intermediate between "molecular" and "ionic" liquids: Liquid Ion Pairs. *Chem. Commun.* **2007**, 3817–3819.

(47) Matsumoto, K.; Hagiwara, R. A New Series of Ionic Liquids Based on the Difluorophosphate Anion. *Inorg. Chem.* **2009**, *48*, 7350–7358.